Optimal Structural Design of Biomorphic Composite Materials*

Ronald H.W. Hoppe[1] and Svetozara I. Petrova[1,2]

[1] Institute of Mathematics, University of Augsburg,
University Str.14, D-86159 Augsburg, Germany
[2] Central Laboratory for Parallel Processing, Bulgarian Academy of Sciences,
Acad. G. Bontchev Str., Block 25A, 1113 Sofia, Bulgaria

Abstract. The production of biomorphic microcellular silicon carbide ceramics from natural grown materials like wood has attracted in the last few years particular interest in the field of biomimetics. Based on the constitutive microstructural model for the inelastic behavior of the new ceramic composites the macroscale model is obtained by using the homogenization approach. The paper comments on the optimal distribution of our composite material in a suitable reference domain which can carry given loads. The structural optimization problem is solved under a set of constraints on the state variables (displacements) and design parameters (material density and angle of cell rotation). Primal–dual Newton–type interior–point method with proper optimality criteria is applied to the resulting nonconvex nonlinear optimization problem.

1 Introduction

Biotemplating is a new technology in the field of biomimetics that focuses on a material synthesis of biologically grown materials into microcellular ceramic composites by high temperature processing. The biological structures are often microstructural designed materials with a hierarchical composite morphology revealing outstanding mechanical properties such as high modulus and high tensile strength both on micro and on the macro scale. Special emphasis has been done on the production of biomorphic silicon carbide (SiC)-based ceramics from wood (cf., e.g., [4,5] and the references therein). Experiments show that their anisotropic porous microstructures are one-to-one pseudomorphous to the original wood material.

The production process of the biomorphic SiC ceramic materials comprises several processing steps ranging from the preparation of appropriate carbonized preforms by drying and high-temperature pyrolysis (800-1800°C) in inert atmosphere via chemical reactions by liquid- or gaseous-phase Si-infiltrations at 1600°C to postprocessing such as cutting and etching. In this way, the natural

* This work has been partially supported by the German National Science Foundation (DFG) under Grant No.HO877/5-1. The second author has also been supported in part by the Bulgarian NSF Grant I1001/2000.

microstructure can be preserved to produce high performance ceramics with excellent structural-mechanical and thermomechanical properties offering a wide range of applications (heat insulation, particle filters, medical implants, automotive tools, etc.)

Optimal performances of the new composite materials can be obtained by tuning microstructural geometrical features that strongly influence the macrocharacteristics of the final products. Our macroscale model is obtained by using the homogenization approach which has found a lot of applications in mechanics of composite materials (see [1,3,9]). We assume a periodical distribution of the composite microstructure treated as infinitesimal square tracheidal periodicity cell consisting of two materials (carbon and SiC) and a void (no material). Detailed description of the macroscopic homogenized model obtained by asymptotic expansion of the solution of the nonhomogenized elasticity equation with a scale parameter close to zero is given in [6]. In the case of stationary microstructure we compute the effective elasticity coefficients numerically by finite element discretization of the cell. Efficient iterative solvers for the homogenized equation in a linearly elastic design macrostructure are proposed in [7].

In this paper, we focus on the development of efficient methods for the structural optimization of biomorphic microcellular SiC ceramics using homogenization modelling and model validations by experimental studies. The optimal design of microstructural materials by homogenization method is well established in structural mechanics (cf., e.g., [2,10]). The structural optimization problem applied to our macroscopic homogenized model is solved under a set of equality and inequality constraints on the state variables (displacements) and the design parameters (material density and angle of cell rotation). This task typically leads to nonconvex nonlinear minimization problem for the objective functional exhibiting a variety of local optima and saddle points. The behavior of the homogenized elasticity coefficients with respect to the design parameters is investigated and visualized in Section 2. The primal–dual Newton–type interior–point method for solving the optimization problem is applied in Section 3.

2 Design Parameters

Consider a two–dimensional bounded domain Ω of a macroscopic length L occupied by a SiC-based ceramic composite material. We assume periodically distributed constituents with a square periodicity cell Y of characteristic length l consisting of an interior part (region V) that is either void (no material) or filled with silicon surrounded by a layer of silicon carbide (region SiC) and an outer layer of carbon (region C) (see Fig. 1).

Introducing $x \in \Omega$ and $y \in Y$ as the macroscopic (slow) and microscopic (fast) variables and $\varepsilon := l/L$ as the scale parameter, the homogenized approach based on a double scale asymptotic expansion results (see [6] for details) in the homogenized elasticity tensor $\mathbf{E}^H = (E^H_{ijkl}),\ i,j,k,l = 1,2$ of the form

$$E^H_{ijkl} = \frac{1}{|Y|} \int_Y \left(E_{ijkl}(y) - E_{ijpq}(y) \frac{\partial \xi^{kl}_p}{\partial y_q} \right) dy, \tag{1}$$

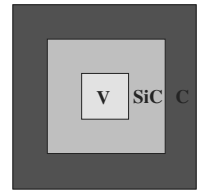

Fig. 1. The periodicity cell $Y = V \cup SiC \cup C$

where $\xi^{kl} = \xi^{kl}(y_1, y_2) \in [H^1(Y)]^2$ is a Y-periodic function which is considered as a microscopic displacement field for the following elasticity cell–problem given in a weak formulation

$$\int_Y \left(E_{ijpq}(y) \frac{\partial \xi_p^{kl}}{\partial y_q} \right) \frac{\partial \phi_i}{\partial y_j} \, dy = \int_Y E_{ijkl}(y) \frac{\partial \phi_i}{\partial y_j} \, dy, \qquad \forall \phi \in V_Y. \tag{2}$$

Here, V_Y is the set of all admissible Y-periodic virtual displacement fields.

Explicit formulas for the homogenized elasticity coefficients (1) can be found only in the case of layered materials and checkerboard structures (cf., e.g., [1,2,9]). Due to the equal solutions $\xi^{12} = \xi^{21}$ one has to solve numerically three problems (2) in the period Y. We use conforming P1 finite elements with respect to a simplicial triangulation of Y taking into account the decomposition $Y = V \cup SiC \cup C$. Note that in our numerical experiments the void is treated as a weak material which is introduced in order to avoid singularity of the stiffness matrix during computations. The values of the Young modulus and Poisson's ratio for the respective materials are given in Table 1.

Table 1. Young's modulus E and Poisson's ratio ν

material	E(GPa)	ν
weak material	0.1	0.45
silicon carbide	410	0.14
carbon	10	0.22

Efficient iterative solvers and extensive numerical experiments for the homogenized equation in a linearly elastic design macrostructure are presented in [7]. The discretized problems have been solved by the PCG method with block- or point-wise incomplete Cholesky decomposition as a preconditioner.

We consider a microstructure occupying the unit cell $Y = [0, 1]^2$. The domain of the weak material in the microcell is specified as a rectangular α by β hole. This choice allows to realize the complete solid ($\alpha = \beta = 0$) and the complete void

($\alpha = \beta = 1$). The remaining values $0 < \alpha < 1$ and $0 < \beta < 1$ characterize the generalized porous medium. The density of the cell is computed by $\mu = 1 - \alpha\beta$.

We have further investigated the dependence of the homogenized elasticity tensor $\mathbf{E}$ on the sizes of the hole in case the carbon has completely reacted with the silicon (i.e., $C = \emptyset$). Figures 2 and 3 present the relations between the effective material properties and the parameters $a = 1 - \alpha$ and $b = 1 - \beta$. Finite element discretization of the cell with 20×20 grid points varying the sizes of the rectangular hole are used to compute the homogenized elasticity coefficients.

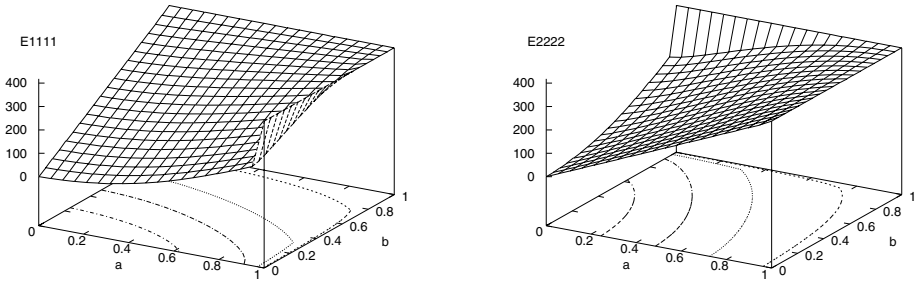

Fig. 2. Homogenized coefficients E_{1111} and E_{2222}

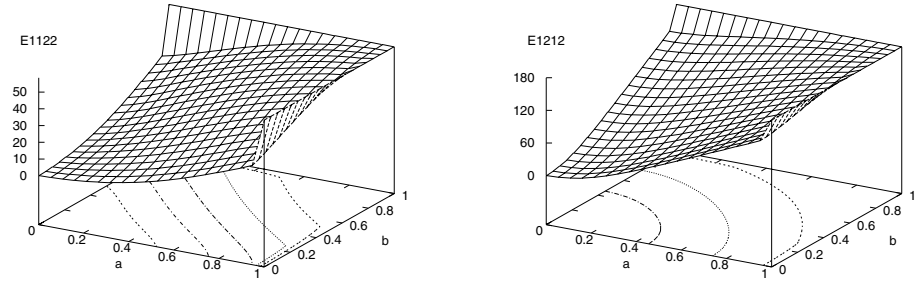

Fig. 3. Homogenized coefficients E_{1122} and E_{1212}

We also note that the homogenized anisotropic elasticity tensor in the macroscale problem strongly depends on the orientation of the microscopic unit cell. Moreover, the influence of rotation of the cell becomes very strong when the size of the microscale hole becomes large. Denote by θ the angle of cell rotation with respect to a fixed reference frame (for instance, the coordinate system). The unrotated case corresponds to $\theta = 0$. The design parameters in the structural otpimization are $\alpha,\ \beta$, and the angle θ. One can compute the rotated elasticity coefficients E^R_{ijkl} for $i, j, k, l = 1, 2$ as follows

$$E^R_{ijkl} = \sum_{m,n,p,q=1}^{2} E^H_{mnpq}(\alpha, \beta)\, R_{im}(\theta)\, R_{jn}(\theta)\, R_{kp}(\theta)\, R_{lq}(\theta), \tag{3}$$

where $R_{im}(\theta),\ 1 \le i, m \le 2$, are the components of the rotation matrix.

In particular, the rotated elasticity tensor $\mathbf{E}^R$ (symmetric) has the form

$$\mathbf{E}^R = \begin{pmatrix} E^R_{1111} & E^R_{1122} & E^R_{1112} \\ E^R_{2211} & E^R_{2222} & E^R_{2212} \\ E^R_{1211} & E^R_{1222} & E^R_{1212} \end{pmatrix},$$

where the corresponding entries depend on the effective elasticity coefficients $E^H_{mnpq} = E^H_{mnpq}(\alpha, \beta)$, $m, n, p, q = 1, 2$ as follows

$$E^R_{1111} = E^H_{1111}\cos^4\theta + E^H_{2222}\sin^4\theta + (4E^H_{1212} + 2E^H_{1122})\sin^2\theta\cos^2\theta,$$

$$E^R_{1122} = (E^H_{1111} + E^H_{2222} - 4E^H_{1212})\sin^2\theta\cos^2\theta + E^H_{1122}(\cos^4\theta + \sin^4\theta),$$

$$E^R_{1112} = \sin\theta\cos\theta\left[(E^H_{1111} - E^H_{1122})\cos^2\theta - (E^H_{2222} - E^H_{1122})\sin^2\theta - 2E^H_{1212}\cos 2\theta\right],$$

$$E^R_{2222} = E^H_{1111}\sin^4\theta + E^H_{2222}\cos^4\theta + (4E^H_{1212} + 2E^H_{1122})\sin^2\theta\cos^2\theta,$$

$$E^R_{2212} = \sin\theta\cos\theta\left[(E^H_{1111} - E^H_{1122})\sin^2\theta - (E^H_{2222} - E^H_{1122})\cos^2\theta + 2E^H_{1212}\cos 2\theta\right],$$

$$E^R_{1212} = (E^H_{1111} + E^H_{2222} - 2E^H_{1122})\sin^2\theta\cos^2\theta + E^H_{1212}\cos^2 2\theta.$$

Figure 4 shows the behavior of the rotated elasticity coefficients for a square hole in the microcell with density $\mu = 0.8$ and $\mu = 0.26$, respectively. We vary the angle of cell rotation by values $0 \le \theta \le 1.5$ given in radians. Note that for a square cell the profile of the coefficient E_{1111} coincides with those of E_{2222}.

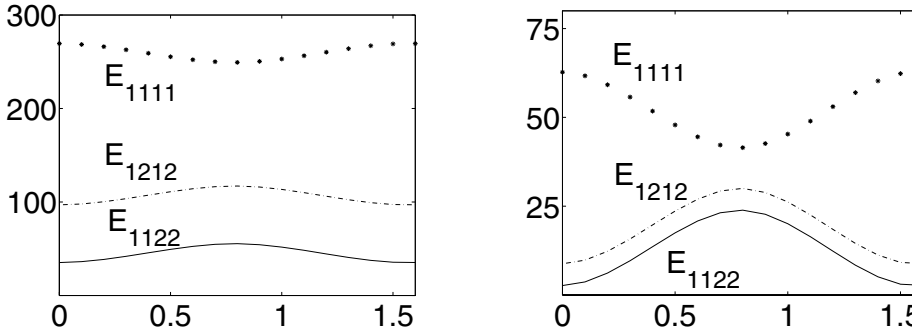

Fig. 4. Elastic coefficients w.r.t. to cell rotation (density $\mu = 0.8$ and $\mu = 0.26$)

Figure 5 displays the dependence of the homogenized elasticity coefficients on the density of the cell. We consider a square hole and compute the effective elasticity tensor for a certain number of points of the density (varying the size of the hole). In order to get a continuous variation with respect to the material density, the remaining values of the homogenized elasticity coefficients on

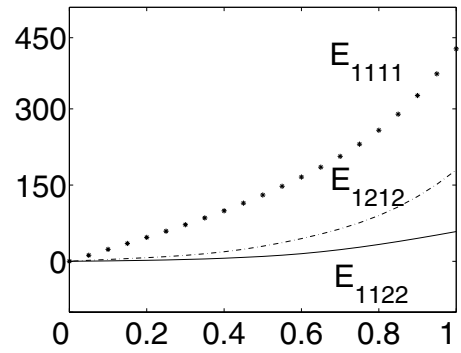

Fig. 5. Elastic coefficients w.r.t. density (square hole)

Figure 5 are interpolated by splines. One can easily observe a highly nonlinear behavior of these coefficients.

Our purpose now is to form continuous functions for the corresponding material coefficients E^H_{ijkl}. We note that E^H_{ijkl} are computed only for a fixed number of values of the cell hole sizes and interpolated by, for instance, Legendre polynomials or Bezier curves defined in the interval $[0, 1]$ to obtain a continuous functional dependence. Thus, together with the expressions (3) we compute the rotated homogenized elasticity tensor $\mathbf{E}^R$, depending on sines and cosines in θ. Concerning the optimization problem the continuous functions of the rotated material coefficients allow us to compute explicitly the gradient and Hessian of the Lagrangian function needed in the optimization loops.

3 The Optimization Problem

In this section, we consider the problem to compute the optimal distribution of our composite material in a given domain. Let $\Omega \subset \mathcal{R}^2$ be a suitable chosen domain that allows to introduce surface traction $\mathbf{t}$ applied to $\Gamma_T \subset \partial\Omega$. On the remaining portion Γ_D of the boundary the displacements $\mathbf{g}$ are specified. We assume a design composite with a square hole which is advantageous to use just one variable in the optimization problem for the material distribution.

We consider the mean compliance of the structure defined as follows

$$J(\mathbf{u}, \alpha) = \int_\Omega \mathbf{f} \cdot \mathbf{u}\, dx + \int_{\Gamma_T} \mathbf{t} \cdot \mathbf{u}\, ds, \tag{4}$$

where $\mathbf{f}$ is the external body force applied to Ω. The displacement vector $\mathbf{u} = (u_1, u_2)^T$ represents the state variables, and the vector $\alpha = (\mu, \theta)^T$ stands for the design parameters (μ - the density of the composite material and θ - the angle of rotation).

For a given volume of material M our structural optimization problem has the form

$$\inf_{\mathbf{u},\alpha} J(\mathbf{u}, \alpha),$$

subject to the following equality and inequality constraints

$$\sum_{i,j,k,l=1}^{2} \int_{\Omega} E^R_{ijkl} \frac{\partial u_k}{\partial x_l} \frac{\partial \phi_i}{\partial x_j}\, dx = \int_{\Omega} \mathbf{f} \cdot \phi \, dx + \int_{\Gamma_T} \mathbf{t} \cdot \phi \, ds, \qquad \forall \phi \in V_0 \tag{5}$$

$$g(\mu) := \int_{\Omega} \mu \, dx = M\,, \qquad \mu_1 \le \mu \le \mu_2, \tag{6}$$

for constants $0 \le \mu_1 < \mu_2 \le 1$. Note that (5) is the weak form of the rotated homogenized equilibrium equation. Here, $\mathbf{u} \in V_D = \{\mathbf{v} \in \mathbf{H}^1(\Omega) | \mathbf{v} = \mathbf{g} \text{ on } \Gamma_D\}$ and $V_0 = \{\mathbf{v} \in \mathbf{H}^1(\Omega) | \mathbf{v} = \mathbf{0} \text{ on } \Gamma_D\}$.

Furthermore, the state variables are discretized by conforming P1 elements with respect to a triangulation of Ω. The discretized nonlinear constrained minimization problem has the following form

$$\inf_{\mathbf{u},\mu,\theta} J(\mathbf{u}, \mu, \theta), \tag{7}$$

subject to

$$\begin{aligned} A(\mu,\theta)\,\mathbf{u} - \mathbf{b} &= 0, \\ \mu - \mu_1 &\ge 0, \\ \mu_2 - \mu &\ge 0, \end{aligned} \tag{8}$$

where $A(\mu, \theta)$ is the stiffness matrix corresponding to (5) and $\mathbf{b}$ is the discrete load vector.

The discretized constrained minimization problem is solved by primal–dual interior–point method substituting the inequality constraints in (8) by logarithmic barrier functions. Assuming that $\mu > \mu_1$ and $\mu_2 > \mu$ this substitution results in the following parametrized family of optimization subproblems

$$\inf_{\mathbf{u},\mu,\theta} \left[J(\mathbf{u}, \mu, \theta) - \rho \, (\log(\mu - \mu_1) + \log(\mu_2 - \mu)) \right] \tag{9}$$

subject to

$$A(\mu, \theta)\,\mathbf{u} - \mathbf{b} = 0, \tag{10}$$

where $\rho > 0$ is a suitably chosen barrier parameter. Coupling the equality constraint by Lagrangian multiplier we have the following Lagrangian function associated with the problem (9)-(10)

$$\begin{aligned} L_\rho(\mathbf{u}, \mu, \theta; \lambda) := {} & J(\mathbf{u}, \mu, \theta) - \rho \, (\log(\mu - \mu_1) + \log(\mu_2 - \mu)) \\ & + \lambda^T (A(\mu, \theta)\,\mathbf{u} - \mathbf{b}). \end{aligned}$$

The first-order Karush–Kuhn–Tucker (KKT) conditions are given by

$$\mathbf{F}^\rho(\mathbf{u}, \mu, \theta; \lambda) = \mathbf{0}\,, \tag{11}$$

where

$$\begin{aligned} F_1^\rho &= \nabla_{\mathbf{u}} L_\rho = \nabla_{\mathbf{u}} J + A(\mu,\theta)^T \lambda\,, \\ F_2^\rho &= \nabla_{\mu} L_\rho = \partial_\mu(\lambda^T A(\mu,\theta)\mathbf{u}) - \rho/d_1 + \rho/d_2\,, \\ F_3^\rho &= \nabla_{\theta} L_\rho = \partial_\theta(\lambda^T A(\mu,\theta)\mathbf{u})\,, \\ F_4^\rho &= \nabla_{\lambda} L_\rho = A(\mu,\theta)\,\mathbf{u} - \mathbf{b}\,, \end{aligned} \tag{12}$$

and $d_1 := \mu - \mu_1$ and $d_2 := \mu_2 - \mu$. Since for $\rho \to 0$ the expressions ρ/d_1 and ρ/d_2 approximate the complementarity conditions associated with (7), it is standard to introduce $z := \rho/d_1 \geq 0$ and $w = \rho/d_2 \geq 0$ serving as perturbed complementarity. Then, the primal–dual Newton–type interior–point method is applied to three sets of variables: primal feasibility $(\mathbf{u}, \mu, \theta)$, dual feasibility (λ), and perturbed complementarity conditions related to (z, w).

Denote the Lagrangian function of problem (7)-(8) by

$$\begin{aligned} L(\mathbf{u}, \mu, \theta; \lambda; z, w) := & J(\mathbf{u}, \mu, \theta) \\ & + \lambda^T (A(\mu, \theta)\, \mathbf{u} - \mathbf{b}) \\ & - z(\mu - \mu_1) - w(\mu_2 - \mu). \end{aligned}$$

Taking into account the KKT conditions the Newton method results in

$$\begin{pmatrix} 0 & L_{\mathbf{u}\mu} & L_{\mathbf{u}\theta} & L_{\mathbf{u}\lambda} & 0 & 0 \\ L_{\mu\mathbf{u}} & L_{\mu\mu} & L_{\mu\theta} & L_{\mu\lambda} & -1 & 1 \\ L_{\theta\mathbf{u}} & L_{\theta\mu} & L_{\theta\theta} & L_{\theta\lambda} & 0 & 0 \\ L_{\lambda\mathbf{u}} & L_{\lambda\mu} & L_{\lambda\theta} & 0 & 0 & 0 \\ 0 & z & 0 & 0 & d_1 & 0 \\ 0 & -w & 0 & 0 & 0 & d_2 \end{pmatrix} \begin{pmatrix} \triangle \mathbf{u} \\ \triangle \mu \\ \triangle \theta \\ \triangle \lambda \\ \triangle z \\ \triangle w \end{pmatrix} = - \begin{pmatrix} \nabla_{\mathbf{u}} L \\ \nabla_{\mu} L \\ \nabla_{\theta} L \\ \nabla_{\lambda} L \\ \nabla_{z} L \\ \nabla_{w} L \end{pmatrix}, \tag{13}$$

where $\nabla_z L = d_1 z - \rho$ and $\nabla_w L = d_2 w - \rho$. The coefficient matrix (13) is usually referred to as the primal–dual system. It can be easily symmetrized but we do not use this approach here. Instead we eliminate the increments $\triangle z$ and $\triangle w$ yielding the condensed primal–dual system

$$\begin{pmatrix} 0 & L_{\mathbf{u}\mu} & L_{\mathbf{u}\theta} & L_{\mathbf{u}\lambda} \\ L_{\mu\mathbf{u}} & \tilde{L}_{\mu\mu} & L_{\mu\theta} & L_{\mu\lambda} \\ L_{\theta\mathbf{u}} & L_{\theta\mu} & L_{\theta\theta} & L_{\theta\lambda} \\ L_{\lambda\mathbf{u}} & L_{\lambda\mu} & L_{\lambda\theta} & 0 \end{pmatrix} \begin{pmatrix} \triangle \mathbf{u} \\ \triangle \mu \\ \triangle \theta \\ \triangle \lambda \end{pmatrix} = - \begin{pmatrix} \nabla_{\mathbf{u}} L \\ \tilde{\nabla}_{\mu} L \\ \nabla_{\theta} L \\ \nabla_{\lambda} L \end{pmatrix}, \tag{14}$$

where $\tilde{L}_{\mu\mu} := L_{\mu\mu} + z/d_1 + w/d_2$ and $\tilde{\nabla}_{\mu} L := \nabla_{\mu} L - \nabla_z L/d_1 + \nabla_w L/d_2$. For details of solving the condensed primal–dual system by interior–point method using damped Newton iterations in structural optimization of electromagnetic devices we refer to [8].

References

1. Bakhvalov, N., Panasenko, G.: Averaging Processes in Periodic Media. Nauka, Moscow (1984)
2. Bendsøe, M.P.: Optimization of Structural Topology, Shape, and Material. Springer (1995)
3. Bensoussan, A., Lions, J.L., Papanicolaou, G.: Asymptotic Analysis for Periodic Structures. North–Holland, Elsevier Science Publishers, Amsterdam (1978)
4. Greil, P., Lifka, T., Kaindl A.: Biomorphic cellular silicon carbide ceramics from wood: I. Processing and microstructure. J. Europ. Ceramic Soc. 18 (1998) 1961–1973.

5. Hoffmann, C., Vogli, E., Kladny, R., Kaindl, A., Sieber, H., Greil, P.: Processing of biomorphic ceramics from wood. In: Stanzl-Tschegg, S.E. et al. (eds.): Proc. 1st Int. Symp. on Wood Mechanics, Vienna (2000) 221–229.
6. Hoppe, R. H.W., Petrova, S. I.: Structural optimization of biomorphic microcellular ceramics by homogenization approach. In: Margenov, S., Wasniewski, J., and Yalamov, P. (eds.): Large-Scale Scientific Computing. Lecture Notes in Computer Science, Vol. 2179, Springer-Verlag (2001) 353–360.
7. Hoppe, R. H.W., Petrova, S. I.: Homogenized elasticity solvers for biomorphic microcellular ceramics. In: Brezzi. F. et al. (eds.): Proc. ENUMATH 2001, July 23-28, 2001, Ischia, Italy, Springer ITALIA (to appear).
8. Hoppe, R. H.W., Petrova, S. I., Schulz, V.: Primal–dual Newton–type interior–point method for topology optimization. J. Optim. Theory Appl. 114 (2002) 545–571.
9. Jikov, V.V., Kozlov, S.M., Oleinik, O.A.: Homogenization of Differential Operators and Integral Functionals. Springer (1994)
10. Suzuki, K., Kikuchi, N.: A homogenization method for shape and topology optimization. Comput. Meth. Appl. Mech. Engrg. 93 (1991) 291–318.